Structural connectivity mapping and parcellation of the human subthalamic nucleus using ultra-high field diffusion MRI

Birgit Renske Plantinga[1,2], Alard Roebroeck[3], Matteo Bastiani[3], Valentin Gereon Kemper[3], Maartje Melse[1], Kâmil Uludag[3], Mark Kuijf[4], Ali Jahanshahi[1], Bart ter Haar Romenij[2], and Yasin Temel[1,5]

[1]Department of Neuroscience, Maastricht University, Maastricht, Limburg, Netherlands, [2]Biomedical Image Analysis, Eindhoven University of Technology, Eindhoven, Noord-Brabant, Netherlands, [3]Department of Cognitive Neuroscience, Maastricht University, Maastricht, Limburg, Netherlands, [4]Department of Neurology, Maastricht University Medical Center, Maastricht, Limburg, Netherlands, [5]Department of Neurosurgery, Maastricht University Medical Center, Maastricht, Limburg, Netherlands

Target audience

Neuroscientists, neurosurgeons, and neurologists interested in high resolution MR basal ganglia anatomy

Purpose

The subthalamic nucleus (STN) is a relatively small deep brain structure that is involved in motor, limbic, and associative processes[1]. Deep brain stimulation (DBS) of the STN is used to treat basal ganglia disorders such as Parkinson's disease and obsessive compulsive disorder[2,3]. Good clinical outcome requires the targeting of either the motor or the limbic part of the STN, respectively. Although the STN can be well delineated at ultra-high field MRI[4], with current clinical imaging techniques it is not possible to derive its functional zones due to its small size (around 106 mm^3 [3 5]), which typically only comprises a few voxels (size 2 × 2 × 2 mm^3 [3 6]). In this study we investigate the structural connectivity profile to parcellate the STN with the aid of ultra-high field *ex vivo* MRI at very high spatial resolution.

Methods

A human post mortem specimen originally kept in formalin, including the left STN, substantia nigra, red nucleus, and globus pallidus, was scanned in PBS using a 7 T MRI scanner (Magnetom 7 T, Siemens). The protocol consisted of two scans: a) 0.3 mm nominal isotropic resolution, gradient echo (GRE) imaging (TE = 11 ms, TR = 37 ms), and b) 0.5 mm isotropic resolution diffusion weighted segmented spin echo 3D EPI (TE = 60 ms, TR = 500 ms, 60 diffusion directions and 8 b0s, b-value = 2800 s/mm^2, total scan time = 65 hours). After FSL's eddy current and motion correction[7], constrained spherical deconvolution-based probabilistic fiber tracking was performed on the whole specimen (2,313,310 tracks) with MRtrix[8] (parameters: step size = 0.05 mm, minimum curvature = 0.1 mm, FOD amplitude cutoff = 0.3, FOD amplitude cutoff for initiation = 0.01) from which only the fibers intersecting the STN (65,182 tracks) were subsequently filtered. The included basal ganglia nuclei and white matter bundles were manually delineated with ITK-SNAP[9]. The relative number of fibers connected to each region as well as the origin of these fibers within the STN (expressed as the percentage of fibers of each voxel connected to that specific region) were computed.

Results

An overview of the projection sites of the STN and their abbreviations is shown in Table 1. Only structures receiving more than 1 % of the STN fibers are listed. Figure 1 shows the origin of these fiber bundles within the STN. This shows that the large amount of fibers that follow the ascending IC mainly originate in the posterior and dorsal parts of the STN. Fibers to the SN originate in the ventrolateral posterior part of the STN. Many projections are also found towards both the GPe and the GPi. Although there is overlap, the anteromedial STN gives rise to more projections to the *anterior* GPe and in the posterolateral STN originate more connections to the *posterior* GPe. The majority of the fibers to the GPi (99 %) run through the anterior half of the GPi (vs. 23 % through the posterior half) and originate in the anteromedial tip of the STN. The STN is also connected to the brain stem, with 17 % of the fibers following the ML, which mainly originate in the ventrolateral part of the STN. Finally, 10 % of the fibers run in lateral direction along the course of the sublenticular part of the IC, which mainly originate in the medial part of the STN. Figure 2 displays the connectivity profile within the SN. Although a similar amount of fibers cross both the SNc and SNr, in the SNc these comprise a bigger volume.

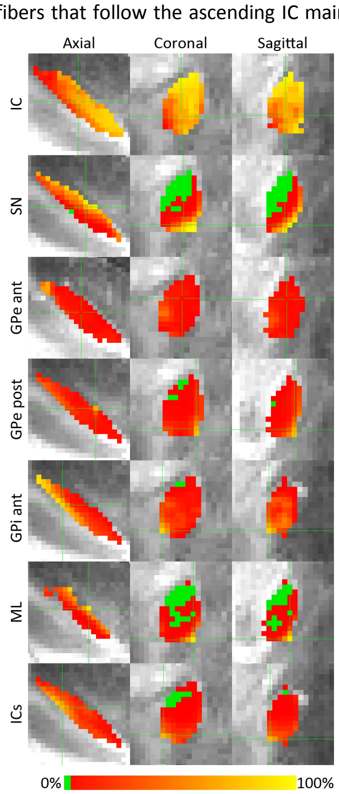

Figure 1. Percentage of fibers per voxel that are connected to the specified region overlaid on the STN (green = no connection).

Table 1. Overview of the projection sites of the STN, with the percentage of all fibers through the STN that project onto it. Individual fibers may intersect multiple structures.

Site	Full name	%
STN	Subthalamic nucleus	100
IC	Internal capsule	30
SN	Substantia nigra:	17
SNc	SN pars compacta	15
SNr	SN pars reticulata	14
GP	Globus pallidus:	14
GPe	External GP	9
GPi	Internal GP	8
ML	Medial lemniscus	9
ICs	Sublenticular IC	5

Discussion

Because fibers that coursed towards but did not fully reach the identified nuclei were discarded, the percentages in Table 1 might be underestimated. Nevertheless, the strong posterior dorsal connection of the STN to the IC and the connection of the medial tip of the STN to the anterior GPi indicate the existence of a gradual division between the motor and limbic parts of the STN, respectively. The posterior and dorsal part is putatively primarily involved in motor processes and the medial side in limbic processes. Furthermore, the STN-SNc connection appears stronger than the STN-SNr connection, which is in contradiction to rodent studies[10]. This suggests that the STN-SNc connection in humans may be more pronounced than what is currently assumed. Although more specimens should be analyzed to assess the reliability of this segregation, these findings may aid in improving clinical pre-operative targeting of DBS patients.

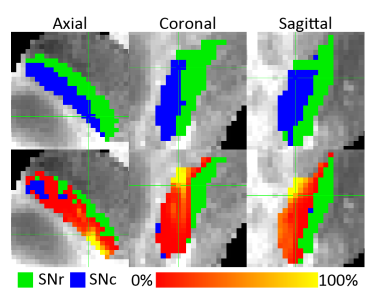

Figure 2. Destination in the SN of fibers connecting to the STN. The upper row shows the manual division of the SN.

References

[1] Temel, Y., et al., Prog Neurobiol, 2005. 76(6): p. 393-413. [2] Benabid, A.L., et al., Lancet Neurol, 2009. 8(1): p. 67-81. [3] Chabardes, S., et al., World Neurosurg, 2013. 80(3-4): p. S31 e1-8. [4] Abosch, A., et al., Neurosurgery, 2010. 67(6): p. 1745-56; discussion 1756. [5] Massey, L.A., et al., Neuroimage, 2012. 59(3): p. 2035-44. [6] Brunenberg, E.J.L., et al., PLoS One, 2012. 7(6): p. e39061-e39061. [7] Jenkinson, M., et al., Neuroimage, 2012. 62(2): p. 782-90. [8] Tournier, J.-D., et al., Int. J. Imaging Syst. Technol., 2012. 22(1): p. 53-66. [9] Yushkevich, P.A., et al., Neuroimage, 2006. 31(3): p. 1116-28. [10] Benazzouz, A., et al., Neurosci Lett, 1995. 189(2): p. 77-80.